



# Numerical study of the effect of non-uniformly perfused tumor on heat transfer in women's breast during menstrual cycle under cold environment

Akshara Makrariya<sup>1</sup> · K. R. Pardasani<sup>2</sup>

Received: 8 September 2018 / Revised: 22 April 2019 / Accepted: 23 April 2019 / Published online: 11 May 2019  
© Springer-Verlag GmbH Austria, part of Springer Nature 2019

## Abstract

In this paper, a model is proposed for heat transfer in women's breast with and without non-uniformly perfused tumour during menstrual cycle under cold environment. The important biophysical parameters like blood flow, metabolic activity and thermal conduction have been incorporated in the model. The physical condition of heat loss from outer surface of women's breast exposed to environment has been used to frame boundary conditions. The model is proposed for a two-dimensional hemi-spherical shaped women's breast. The triangular ring elements have been employed to discretize the region. The numerical solution is obtained for a steady-state case by finite element method. The effect of non-uniformly perfused tumor in women's breast during different phases of menstrual cycle has been studied with the help of numerical results. It is concluded that the thermal stress due to malignant tumor in woman's breast gets enhanced due to different phases of menstrual cycle and this information will be useful for developing more effective protocols of thermography for detection of tumors. Such models can be developed further to study the heat transfer processes in the women's breast due to various malignant and benign changes.

**Keywords** Cold environment · Menstrual cycle · Perfused tumor

**Mathematical subject classification** 92B05 · 62P10

## 1 Introduction

The heat transfer processes like heat conduction and heat convection due to blood flow in tissues play an important role in thermoregulation of human body organs by maintaining balance between heat generation and heat loss from the body. The various environmental and physiological conditions affect these heat transfer processes. The present study is confined to estimation of thermal stress in women's breast due to a non-uniformly perfused tumor (Saraswati et al. 2014). The mechanism of thermal interaction of arterial and venous blood plays an important role in thermal

balance of women's breast. The arterial and venous blood temperature varies along flow direction with the angular position in the breast.

In general, Pennes' bio-heat equation is used to model the temperature distribution in the human body tissues. Various other models suggested have been reported as an improvement to Pennes' model that includes continuum models given by Wulf et al. (1975), and Chen and Holmes et al. (1972). Earlier Patterson (Osman and Afify 1988) made experimental investigations to obtain temperature profiles in the human body tissues. Some theoretical work is reported during the last few decades by Pennes (1984), Chao and Yang (1975), Saraswati et al. (2014), Pardasani and Adlakha (1993), Pardasani and Saxena (1989), Perl (1963) and Cooper and Trezek (1972), Gurung (2009), to study the temperature distribution in the human peripheral region under normal environmental and physiological conditions. Saxena and Pardasani (1994), Pardasani and Adlakha (1991) and Saxena and Arya (1981) made attempts to study problems of temperature distribution in the dermal regions of the

✉ Akshara Makrariya  
aksharahul@gmail.com

<sup>1</sup> School of Advanced Science-Mathematics, VIT Bhopal University, Bhopal, India

<sup>2</sup> Department of Mathematics, MANIT, Bhopal, MP 462003, India

human body involving abnormalities like tumors. Pennes (1948), Patterson (1976), Pardasani and Saxena (1990), Saxena (1983) and Saxena and Bindra (1984) developed thermal models of human limbs for one- and two-dimensional steady-state cases under normal physiological and environmental conditions. Agrawal et al. (2010, 2011, 2014, 2015) and Pardasani et al. (2010) developed one-, two- and three-dimensional finite element models to study thermal patterns in the dermal layers of human limbs with and without tumors. Naik et al. (2016), Naik and Pardasani (2018) used finite element analysis in the problems of calcium diffusion in oocytes. Khanday et al. (2000), Khanday and Saxena (2009), Khanday and Rafiq (2014), Khanday and Hussain (2014), and Khanday et al. (2015) studied thermoregulation in human head and other organs under cold environment. Mittal et al. (2015), Makrariya and Adlakha (2013, 2015), Akshara and Neeru (2017), Saxena and Pardasani (1987), Khanday and Khalid (2017), and Mittal and Ramana (2008) proposed thermal models of the normal and malignant tissues in woman's breast under various conditions. Gonzalez (2011) investigated the metabolic heat generation in breast tumors using infrared images and numerically simulating a simplified breast model and a cancerous tumor. Gonzalez (2016) has presented an overview of theoretical and clinical aspects of thermography emphasizing the need for development of standard procedure to obtain and analyze the thermograms. The lack of these standard procedures is one of the bottlenecks that is making thermography a commonly used technique. Gonzalez (2007) performed thermal simulation of breast tumors of various sizes to determine the range of size and depth of tumor in breast which can be detected with the available thermographic technology.

No theoretical study of effect of non-uniformly perfused tumors on temperature in women's breast during various phases of the menstrual cycle is reported till date. Here a finite element model is proposed to study thermal stress in peripheral layers of women's breast involving non-uniformly perfused tumor in presence and absence of menstrual cycle.

## 2 Mathematical models

It is assumed that the properties are most variable along the radial  $r$  and angular  $\theta$  direction, but almost uniform along azimuthal angle  $\varphi$ . The biophysical properties vary mostly along the radial direction and less along the angular direction. But this variation is almost negligible along the azimuthal angle  $\varphi$  as compared to other directions. Thus 3D problem can be modeled as 2D problem assuming that the heat flow and temperature distribution along  $\varphi$  direction is almost uniform. But this temperature distribution varies along radial and angular direction  $\theta$ . This model assumption is also based on our focus of study which is aimed to analyze

the temperature distribution along radial and angular direction as the variation in temperature distribution along radial and angular direction are more significant as compared to azimuthal angle  $\varphi$ .

The partial differential equation for heat flow in peripheral tissues of women's breast for a two-dimensional steady-state case is given by Jas and Pardasani (2000):

$$\frac{1}{r^2} \frac{\partial}{\partial r} \left( Kr^2 \frac{\partial T}{\partial r} \right) + \frac{1}{r^2 \sin \theta} \frac{\partial}{\partial \theta} \left( K \sin \theta \frac{\partial T}{\partial \theta} \right) + m_b c_b (T_b - T) + S + W = 0. \quad (1)$$

Here,  $K$ ,  $m_b$ ,  $c_b$ ,  $T_b$ ,  $T$ ,  $S$  and  $W$  are the coefficients of thermal conductivity of tissue, blood mass flow rate, specific heat of blood, blood temperature, tissue temperature at position  $r$ , rate of controlled and uncontrolled metabolic heat generation, respectively. The heat loss due to conduction, convection, radiation, and evaporation at the outer surface of women's breast exposed to the environment is expressed as the following boundary condition:

$$-K \frac{\partial T}{\partial r} = h(T - T_a) + LE \text{ at } r = r_n, \theta \in (0, \pi), \quad (2)$$

where  $h$ ,  $T_a$ ,  $L$  and  $E$  are the coefficients of heat transfer, atmospheric temperature, latent heat and rate of sweat evaporation, respectively. The tissue temperature varies along radial and angular direction. The tissue temperature is higher near the core of the breast and lower at the surface of the breast. So the gradient between arterial blood temperature will be less near the core of the breast and higher near the surface of the breast. The tissue temperature in the region of the breast having arteries is at the higher temperature while the tissue temperatures in the region of breast having veins will be at the slightly low temperature. Therefore, the geometry has effect on heat transfer due to blood tissues interfaces. During low environmental temperature, the temperature of inner shell of women's breast varies along angular direction  $\theta$  and can be expressed as following boundary condition:

$$T(r_0, \theta) = F(\theta), \quad F(\theta) = a_1 + a_2\theta + a_3\theta^2. \quad (3)$$

The other form of expression in terms of exponential, trigonometric, and transcendental functions can also be constructed in place of Eq. (3). However, there the focus is on using simplest mathematical expressions to represent the physical phenomenon.

The value of constants  $a_1$ ,  $a_2$ , and  $a_3$  are found by using the conditions:

$$T(r_0, \theta) = \alpha \text{ at } \theta = 0, \quad T(r_0, \theta) = \beta \text{ at } \theta = \pi/2, \\ T(r_0, \theta) = \gamma \text{ at } \theta = \pi,$$

where  $\alpha$  and  $\gamma$  represents the temperatures of location of shell from where the arteries are passing and therefore taken

to be equal to the body core temperature.  $\beta$  is found to be lower than  $\alpha$ , and  $\gamma$  during low atmospheric temperatures.

The variational form of Eq. (1) with the boundary conditions is given by:

$$I^{(e)} = \frac{1}{2} \iint \left[ K^{(e)} r^2 \left( \frac{\partial T^{(e)}}{\partial r} \right)^2 + K^{(e)} \left( \frac{\partial T^{(e)}}{\partial \theta} \right)^2 + \left\{ M^{(e)} (T_A^e - T^{(e)})^2 - \bar{S}^{(e)} \right\} r^2 dr d\theta \right], \tag{4}$$

$$+ \frac{\lambda^{(e)}}{2} \int_{\theta_i}^{\theta_k} \left\{ h(T^{(e)} - T_a)^2 + 2LET^{(e)} \right\} r^2 d\theta : e = 1(1)416,$$

where  $e$  tends to no. of element and is defined element 1–416 starting with node 1.

Here  $r_i$  and  $r_j$  are radii of the  $e$ th element.  $K^{(e)}, M^{(e)}, \bar{S}^{(e)}, T_A^{(e)}$  and  $T^{(e)}$  denote the values of  $K, M, \bar{S}, T_A$  and  $T$ , respectively, in  $e$ th layer.  $\lambda^{(e)}$  is 1 for elements along the surface and  $\lambda^{(e)}=0$  otherwise. The peripheral region of the women’s breast is divided into the epidermis, dermis and subcutaneous tissues. The epidermis and subcutaneous tissues are divided in one layer each, whereas the dermis is divided into 11 layers due to non-homogeneity (Table 1). The region is discretized into 416 triangular ring elements (as shown in Fig. 1).

The following bilinear shape function is assumed for variation of temperature within each element:

$$T^{(e)} = c_1^{(e)} + c_2^{(e)} r + c_3^{(e)} \theta, \tag{5}$$

where  $c_1^{(e)}, c_2^{(e)}$ , and  $c_3^{(e)}$  are constants for the  $e$ th element, here

$$T^{(e)} = T_p, p = i, j, k. \tag{6}$$

The integral  $I^{(e)}$  in expression (4) are evaluated for each element using expression (6) and assembled as given below:

$$I = \sum_{e=1}^N I^{(e)}. \tag{7}$$

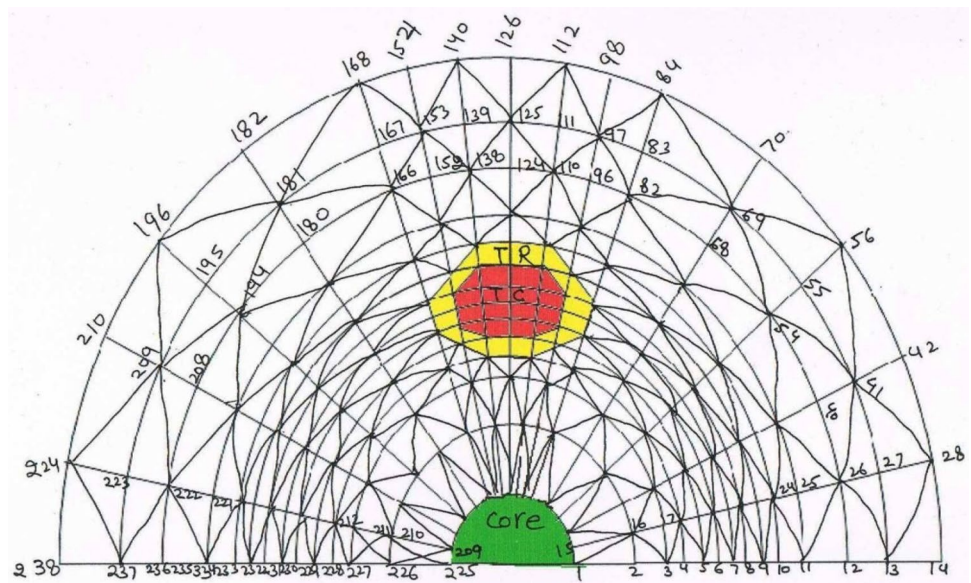
The integral  $I$  is extremized with respect to each nodal temperature  $T_i, i = 1, 2, 3 \dots n$  as given in (1) and it leads to a system of linear algebraic equations as given below:

$$[X]_{n \times n} [T_{n \times 1}] = [Y]_{n \times 1} \tag{8}$$

**Table 1** Triangular ring element information

Element	$i$	$j$	$k$	Type	Element	$i$	$j$	$k$	Type
1	1	16	15	1	27	15	16	29	1
2	1	2	16	1	28	29	16	30	2
3	2	3	16	1	29	16	31	30	1
4	16	3	17	2	30	16	17	31	1
5	3	18	17	1	31	17	18	31	1
6	3	4	18	1	32	31	18	32	2
7	4	5	18	1	33	18	33	32	1
8	18	5	19	2	34	18	19	33	1
9	5	20	19	1	35	19	20	33	1
10	5	6	20	1	36	33	20	34	2
11	6	7	20	1	37	20	35	34	1
12	20	7	21	2	38	20	21	35	1
13	7	22	21	1	39	21	22	35	1
14	7	8	22	1	40	35	22	36	2
15	8	9	22	1	41	22	37	36	1
16	22	9	23	2	42	22	23	37	1
17	9	24	23	1	43	23	24	37	1
18	9	10	24	1	44	37	24	38	2
19	10	11	24	1	45	24	39	38	1
20	24	11	25	2	46	24	25	39	1
21	11	26	25	1	47	25	26	39	1
22	11	12	26	1	48	39	26	40	2
23	12	13	26	1	49	26	41	40	1
24	26	13	27	2	50	26	27	41	1
25	13	28	27	1	51	27	28	41	1
26	13	14	28	1	52	41	28	42	2

**Fig. 1** Finite element discretization of breast region



$X$  and  $Y$  is system of matrices of order  $nx1$  and  $n \times n$ , respectively, and  $\bar{T} = [\bar{T}_1 \bar{T}_2 \bar{T}_3 \dots \bar{T}_n]^T$ . The Gauss elimination method has been used to obtain the solution (8).

### 3 Numerical results and discussion

The numerical results are obtained by Agrawal and Pardasani (2016), Acharya et al. (2016), Saxena and Pardasani (1987) and Viana et al. (2010) using the values of physical and physiological constant given in Table 2.

For a particular sample of peripheral tissue layers,  $r$  is assigned the following values:  $r_1 = 8$  cm;  $r_2 = 8.5$  cm;  $r_3 = 8.54$  cm;  $r_4 = 8.58$  cm;  $r_5 = 8.62$  cm;  $r_6 = 8.66$  cm;  $r_7 = 8.7$  cm;  $r_8 = 8.74$  cm;  $r_9 = 8.78$  cm;  $r_{10} = 8.82$  cm;  $r_{11} = 8.86$  cm;  $r_{12} = 8.9$  cm;  $r_{13} = 9.0$  cm, and  $r_{14} = 9.1$  cm.

Here we take  $W = \eta S$ , which implies that the metabolic activity in tumor is  $\eta$  times of that normal tissues (Table 3). The metabolic activity in tumor varies 7 times of that in normal tissues. As a particular case we take  $\eta = 5.0$ . We observe the effect of variable boundary condition at  $r = 8$  and  $\theta = 0$  to  $\pi$  with temperature  $37^\circ\text{C}$  at  $\theta = 0$  and  $\theta = \pi$  and  $36^\circ\text{C}$  at

$\theta = \pi/2$ . The temperature falls down as we move away from core to the outer skin surface in Figs. 2, 3 and 4. Also the slope of the curve changes at the nodes of epidermis, dermis and subdermal tissues in Fig. 2. This is due to the different properties of each layer. In Figs. 3, 4 the slope of curves changes at the nodes of normal tissues, tumor periphery, and tumor core. This is due to the different properties of tumor core and tumor periphery. There is elevation in temperature profiles is observed at the interface of normal tissues and tumor periphery and then fall in temperature is seen at the interface of tumor periphery and tumor core. There is elevation at the interfaces of tumor core and tumor periphery and then fall in temperature at the interface of tumor periphery and normal tissues. These changes in temperature profiles in the form of elevation and deviation downwards at the various interfaces of normal tissues and tumor give us the idea about the size and location of each layer of tumor and whole tumor. Figures 5 and 6 show temperature differences in spherical shaped woman's breast with non-uniformly perfused tumor due to absence and presence of menstrual cycle. The maximum values of temperature difference in Figs. 5, 6 are, respectively,  $0.21^\circ\text{C}$  and  $0.27^\circ\text{C}$ . The maximum temperature differences in women's breast with tumor

**Table 2** The value for physical and physiological constants (Saxena and Pardasani 1987; Viana et al. 2010)

S. no.	Tissues	K (cal/cm min °C)	$c_b$ (cal/g °C)	S (cal/cm <sup>3</sup> min)	$m_b$ (cal/cm <sup>3</sup> min °C)
1	Bone	0.075	17	0	0
2	Muscle	0.042	3768	0.0684	0.001046
3	Fat	0.016	23	0.058	0.0001880
4	Skin	0.047	368	0.0357	0.003
5	Cysts	0.056	0	0	0

**Table 3** The value for physical and physiological constants for different phases of menstrual cycle (Agrawal and Pardasani 2016; Acharya et al. 2016)

S. no.	Tissues	$m_{b\text{ follicular}}$ (cal/cm <sup>3</sup> min °C)	$m_{b\text{ luteal}}$ (cal/cm <sup>3</sup> min °C)	$S_{\text{ follicular}}$ (cal/cm <sup>3</sup> min)	$S_{\text{ luteal}}$ (cal/cm <sup>3</sup> min)
1	Bone	0	0	0	0
2	Muscle	0.0005	0.0007	0.133	0.1415
3	Fat	0.00009	0.00012	0.0985	0.1135
4	Skin	0.01538	0.02197	0.0665	0.0707
5	Cysts	0	0	0	0

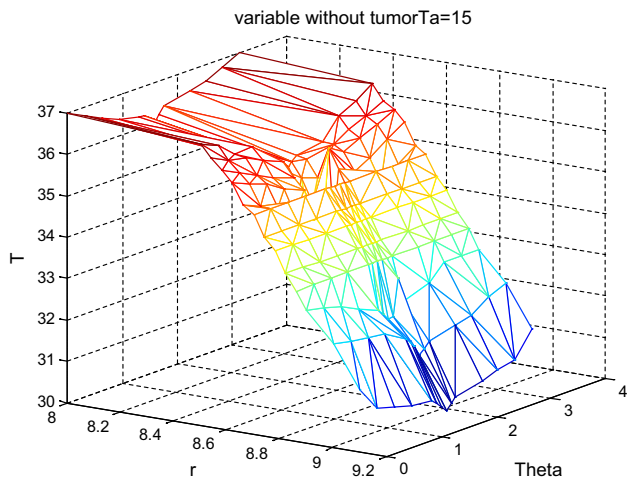


**Fig. 2** Temperature distribution along  $r$  and  $\theta$  direction in female breast with non-uniformly perfused tumor in absence of menstrual cycle for  $T_a = 15^\circ\text{C}$ ,  $E = 0 \text{ gm/cm}^2 \text{ min}$

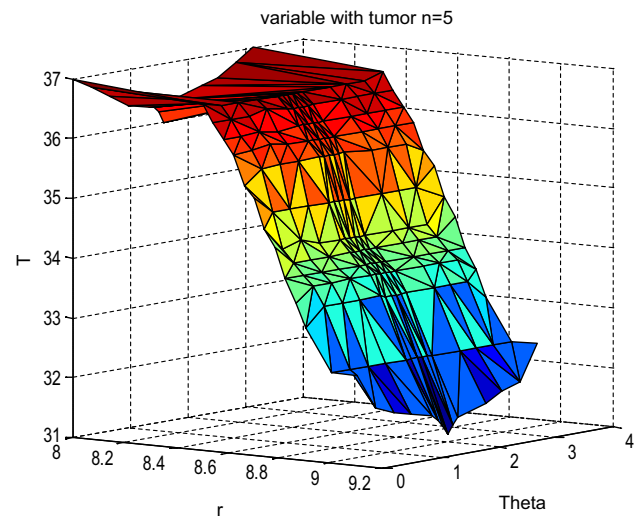


**Fig. 4** Temperature distribution along  $r$  and  $\theta$  direction in female breast with non-uniformly perfused tumor during follicular phase of menstrual cycle for  $T_a = 15^\circ\text{C}$ ,  $E = 0 \text{ gm/cm}^2 \text{ min}$

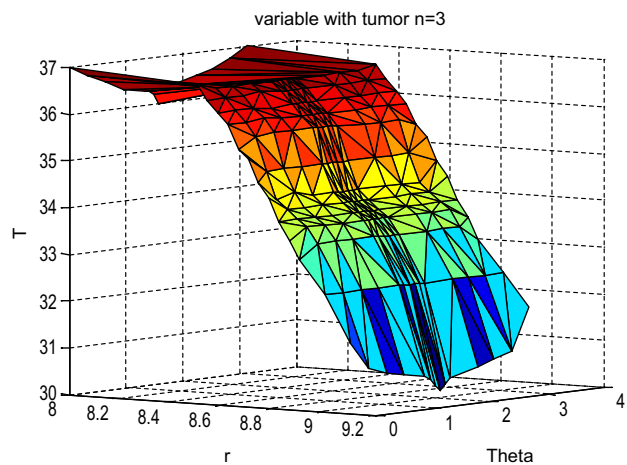


**Fig. 3** Temperature distribution along  $r$  and  $\theta$  direction in female breast with non-uniformly perfused tumor during follicular phase of menstrual cycle for  $T_a = 15^\circ\text{C}$ ,  $E = 0 \text{ gm/cm}^2 \text{ min}$

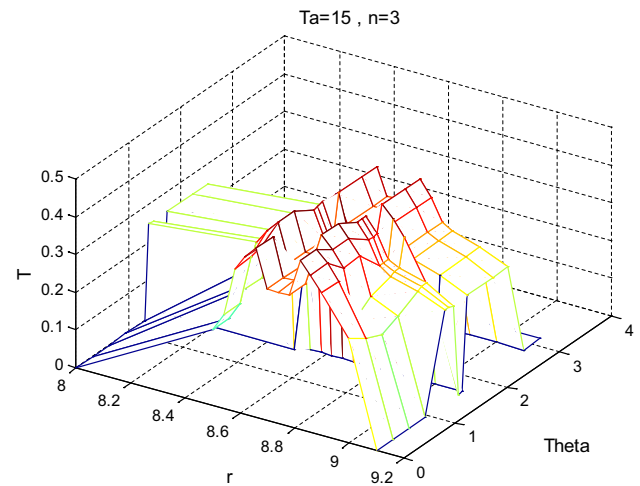


**Fig. 5** Distribution of temperature differences in female breast with non-uniformly perfused tumor between normal condition and follicular phase of menstrual cycle for  $T_a = 15^\circ\text{C}$ ,  $E = 0 \text{ gm/cm}^2 \text{ min}$

due to presence and absence of menstrual cycle is observed in luteal phase of menstrual cycle. Thus, the thermal stress caused by malignant tumor in women’s breast is more in luteal phase than in follicular phase of menstrual cycle. The

information generated regarding the changes in the slopes of the curve at different junctions of tumor and normal tissues can be exploited in thermograms for identification of shape,



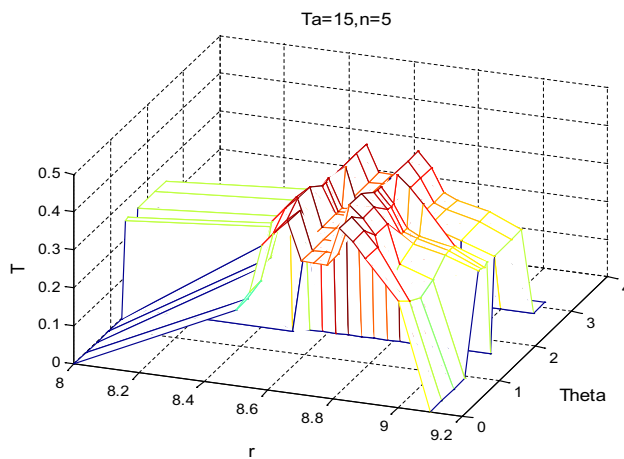


**Fig. 6** Distribution of temperature differences in female breast with non-uniformly perfused tumor between normal condition and luteal phase of menstrual cycle for  $T_a = 15\text{ }^\circ\text{C}$ ,  $E = 0\text{ gm/cm}^2\text{ min}$

size, location and boundaries of various layers of tumors and normal tissues in woman's breast. Further, the enhanced effect of tumors in woman's breast during various phases of menstrual cycle can also be useful in improving protocols for diagnosis of tumors by thermo graphic techniques.

## 4 Conclusions

The finite element model is proposed and employed to estimate the thermal stress due to non-uniformly perfused tumors in peripheral regions of woman's breast during different phases of menstrual cycle under cold environment. From the results it is concluded that the non-uniformly perfused malignant tumor in the woman's breast causes thermal disturbances which vary in quantity, shape of thermal patterns in women's breast and are specific to the type, size, shape and location of tumor. The thermal patterns due to malignant tumor in women's breast also vary due to benign changes caused during follicular and luteal phase of menstrual cycle. The thermal stress due to malignant tumor in women's breast gets enhanced due to benign changes caused during the follicular and luteal phase of menstrual cycle. Therefore, it is concluded that the thermography will be more effective in detection of malignant tumor in women's breast during luteal and follicular phase of menstrual cycle. The triangular ring element-based finite element approach has proved to be quite effective in incorporating the non-homogeneity of the region and variations in biophysical parameters. The proposed model is applicable for benign changes due to various phases of menstrual cycle. However, there are other benign changes occurring in woman's breast due to various causes and can influence the thermal stress in woman's breast due to

malignant tumors and the authors intend to incorporate them in their future studies.

**Acknowledgements** The authors are grateful to Science and Engineering Research Board, Department of Science and Technology, New Delhi, India, for providing assistance for this work under NPDF-Scheme.

## References

- Acharya S, Gurung DB, Saxena VP (2014) Human males and females body thermoregulation: perfusion effect analysis. *J Therm Biol* 45:30–36
- Acharya S, Gurung DB, Saxena VP (2016) Mathematical modeling of sex related differences in the sensitivity of the sweating heat responses to change in body temperature. *Br J Math Comput Sci* 12(4):1
- Agrawal M, Pardasani KR (2016) Finite element model to study temperature distribution in skin and deep tissues of human limbs. *J Therm Biol* 62:98–105
- Agrawal M, Adlakha N, Pardasani KR (2010a) Semi numerical model to study temperature distribution in peripheral layers of elliptical and tapered shaped human limbs. *J Mech Med Biol* 10(1):57–72
- Agrawal M, Adlakha N, Pardasani KR (2010b) Three-dimensional finite element model to study heat flow in dermal region of elliptical and tapered shaped human limbs. *Appl Math Comput* 217(8):4129–4140
- Agrawal M, Adlakha N, Pardasani KR (2011) Finite element model to study thermal effect of uniformly perfused tumor in dermal layers of elliptical shaped human limbs. *Int J Biomath* 4(02):241–254
- Agrawal M, Pardasani KR, Adlakha N (2014) Steady state temperature distribution in dermal regions of an irregular tapered shaped human limb with variable eccentricity. *J Therm Biol* 44:27–34
- Agrawal M, Pardasani KR, Adlakha N (2015) Finite element model to study the thermal effect of tumors in dermal regions of irregular tapered shaped human limbs. *Int J Therm Sci* 98:287–295
- Akshara M, Neeru A (2017) Quantitative study of thermal disturbances due to non uniformly perfused tumors in peripheral regions of women's breast. *J Cancer Inf* 16:1–13
- Chao KN, Yang WJ (1975) Response of skin and tissue temperature in sauna and steam baths. *Bio Mech Symp* 1:69–71
- Cooper TE, Trezek GJ (1972) A probe technique for determining the thermal conductivity of tissue. *ASME J Heat Transf* 94:133–140
- González FJ (2007) Thermal simulation of breast tumors. *Revista Mexicana Física* 53(4):323–326
- González FJ (2011) Non-invasive estimation of the metabolic heat production of breast tumors using digital infrared imaging. *QIRT J* 8(2):139–148
- González FJ (2016) Theoretical and clinical aspects of the use of thermography in non-invasive medical diagnosis. *Biomed Spectrosc Imaging* 5(4):347–358
- Gurung DB (2009) FEM approach to one dimensional unsteady temperature distribution in human dermal parts with quadratic shape function. *J Appl Math Informatics* 27(1-2):301–303
- Gurung DB (2010) Transient temperature distribution in human dermal part with protective layer at low atmospheric temperature. *Int J Biomath* 3(4):439–451
- Jas P, Pardasani KR (2000) Numerical simulation of the effect of polycythemia Vera on heat flow in human dermal regions. *Ind J Pure Appl Math* 31(12):1595–1606
- Khanday MA, Hussain F (2014) Explicit formula of finite difference method to estimate human peripheral tissue temperatures during exposure to severe cold stress. *J Thermal Biol* 48:51–55

- MA Khanday, Khalid N (2017), Mathematical and numerical analysis of thermal distribution in cancerous tissues under the local heat therapy. *Int J Biomath*
- Khanday MA, Najar A (2015) Maclaurin's series approach for the analytical solution of oxygen transport to the biological tissues through capillary bed. *J Med Imaging Health Inf* 5(5):959–963
- Khanday MA, Rafiq A (2014) Variational finite element method to study the absorption rate of drug at various compartments through transdermal drug delivery system. *Alexandria J Med* 51(3):219–223
- Khanday MA, Saxena VP (2009) Finite element approach for the study of thermoregulation in human head exposed to cold environment. *Proc J Am Inst Phys* 1146:375–385
- Khanday MA et al (2015) Finite element approach to study the behaviour of fluid distribution in the dermal regions of human body due to thermal stress. *J Egypt Math Soc* 5:6. <https://doi.org/10.1016/j.joems.2014.12.009>
- Makrariya A, Adlakha N (2013) Two-dimensional finite element model of temperature distribution in dermal tissues of extended spherical organs of a human body. *Int J Biomath* 6(1):1–15
- Makrariya A, Adlakha N (2015) Two-dimensional finite element model to study temperature distribution in peripheral regions of extended spherical human organs involving uniformly perfused tumors. *Int J Biomath* 8:6
- Mittal M, Ramana MP (2008) Breast tumor a simulation and parameters estimation using evolutionary algorithms, Hindvani Publishing Corporation Modeling and Simulation in Engineering. Article ID 756436
- Naik PA, Pardasani KR (2016) Finite element model to study calcium distribution in oocytes involving voltage gated  $Ca_2^+$  channel, ryanodine receptor and buffers. *Alexandria J Med* 52(1):43–49
- Naik PA, Pardasani KR (2018a) Three dimensional finite element model to study effect of RyR calcium channel, ER leak and SERCA pump on calcium distribution in oocyte cell. *Int J Comput Methods* 15(6):1–19
- Naik PA, Pardasani KR (2018b) 2D finite element analysis of calcium distribution in oocytes. *Netw Model Anal Health Inform Bioinform* 7:1–11
- Osman MM (1994) Effect of arterio-venous heat exchange on breast temperature profile. *J Phys III France* 4:435–442
- Osman MM, Afify EM (1984) Thermal modeling of the normal woman's breast. *J Biomech Eng* 106:123–130
- Osman MM, Afify EM (1988) Thermal modeling of the malignant woman's breast. *J Biomech Eng* 110:269–276
- Pardasani KR, Adlakha N (1991) Exact solution to a heat flow problem in peripheral tissue layers with a solid tumor in the dermis. *Indian J Pure Appl Math* 22(8):679–687
- Pardasani KR, Adlakha N (1993) Two dimensional steady state temperature distribution in annular tissues of a human or animal body. *Ind J Pure Appl Math* 24:721–728
- Pardasani KR, Adlakha N (1995) Coaxial circular sector elements to study two-dimensional heat distribution problem in dermal regions of human limbs. *Math Comp Modeling* 22(9):127–140
- Pardasani KR, Saxena VP (1989) Exact solution to temperature distribution problem in annular skin layers. *Bull Calcutta Math Soc* 5:81–108
- Pardasani KR, Saxena VP (1990) Temperature distribution in skin and subcutaneous tissues with a uniformly perfused tumor in the dermis. *Proc Nat Acad Sci* 60:11–20
- Patterson AM (1976) Measurement of temperature profiles in human skin. *South Afr J Sci* 72:79
- Pennes H (1948) Analysis of tissue and arterial blood temperature in the resting human forearm. *J Appl Physiol* 1(2):93–122
- Perl W (1963) Heat and matter distribution equation to include clearance by capillary blood flow. *Ann NY Acad Soc* 108:92–105
- Saraswati A, Gurung DB, Saxena VP (2014) Transient temperature distribution in human males and females body due to variation in perfusion effect. *Int J Appl Math* 29:1263–1270
- Saxena VP (1983) Temperature distribution in human skin and sub dermal tissues. *J Theor Biol* 102:277–286
- Saxena VP, Arya D (1981) Steady state heat distribution in epidermis, dermis and sub dermal tissues. *J Theor Biol* 89:423–432
- Saxena VP, Bindra JS (1984) Steady state temperature distribution in dermal regions of human body with variable blood flow perspiration and self controlled metabolic heat generation. *Indian J Pure Appl Math* 15(1):31–42
- Saxena VP, Pardasani KR (1987) Steady state radial heat flow in skin and underlying tissue of layers of spherical regions of human or animal body. *Ind J Tech* 25:501–505
- Saxena VP, Pardasani KR, Agarwal R (1988) Unsteady state heat flows in epidermis and dermis of human body. *J. Indian. Acad Sci* 98(1):71–80
- Sudharsan NM, Ng EYK, Teh SL (1999) Surface temperature distribution of a breast with and without tumor. *Comput Method Biomech Biomed Eng* 23:187–199
- MJA Viana, FGS Santos, TL Rolim, RCF Lima (2010) Simulating Breast Temperature Profiles through Substitute Geometries from Breast Prostheses. In: IWSSIP 2010—17th International Conference on Systems, Signals and Image Processing. pp 304–307
- V.P Saxena.,and K.R Pardasani, Effect of dermal tumor on temperature distribution in skin with variable blood flow, *Bull. Mathematical Biology, USA* (1991)

**Publisher's Note** Springer Nature remains neutral with regard to jurisdictional claims in published maps and institutional affiliations.